Stochastic DG Placement for Conservation Voltage Reduction Based on Multiple Replications Procedure

Zhaoyu Wang, *Student Member, IEEE*, Bokan Chen, Jianhui Wang, *Senior Member, IEEE*, and Miroslav M. Begovic, *Fellow, IEEE*

***Abstract*—Conservation voltage reduction (CVR) and distributed-generation (DG) integration are popular strategies implemented by utilities to improve energy efficiency. This paper investigates the interactions between CVR and DG placement to minimize load consumption in distribution networks, while keeping the lowest voltage level within the predefined range. The optimal placement of DG units is formulated as a stochastic optimization problem considering the uncertainty of DG outputs and load consumptions. A sample average approximation algorithm-based technique is developed to solve the formulated problem effectively. A multiple replications procedure is developed to test the stability of the solution and calculate the confidence interval of the gap between the candidate solution and optimal solution. The proposed method has been applied to the IEEE 37-bus distribution test system with different scenarios. The numerical results indicate that the implementations of CVR and DG, if combined, can achieve significant energy savings.**

***Index Terms*—Conservation voltage reduction (CVR), distributed generation (DG), Monte Carlo sampling, multiple replications procedure (MRP), sample average approximation (SAA), stochastic programming (SP).**

NOMENCLATURE

$V_{i,y,n}$	Voltage magnitude at node i in scenario n in year y.
r_i/x_i	Line resistance/reactance between nodes i and $i+1$.
$P_{i,y,n}/Q_{i,y,n}$	Active/reactive power flow from node i to $i+1$ in scenario n in year y.
$P^b_{i,y}/Q^b_{i,y}$	Base active/reactive load for the exponential load model at node i in year y.
α_n/β_n	Active/reactive power exponent for the exponential load model in scenario n.
$P^{\text{load}}_{y,n}$	Total active load consumption of the system in scenario n in year y.
$p^l_{i,y,n}/q^l_{i,y,n}$	Active/reactive load consumption at node i in scenario n in year y.
T_{fc}/T_{fh}	Cooling/heating reference temperature.
$T_{i,y,n}$	Temperature at node i in scenario n in year y.
μ/γ	Parameters for active/reactive load regression model with regard to temperature.
$p^{g,wt}_{i,y,n}/p^{g,pv}_{i,y,n}$	Active power output of the WT/PV generator at node i in scenario n in year y.
$q^g_{i,y,n}$	Reactive power generation at node i in scenario n in year y.
Q^C_i	Size of capacitor at node i.
$X^C_{i,y,n}$	Switch on (1)/off (0) status of the capacitor at node i in scenario n in year y.
a^{wt}_i/a^{pv}_i	0 if there is no WT/PV at node i and 1 if there is a WT/PV at node i.
$\omega^{wt}_{i,y,n}/\omega^{pv}_{i,y,n}$	Stochastic WT/PV output of one discrete increment at node i in scenario n in year y.
s^{wt}/s^{pv}	One discrete increment of WT/PV size (in megavolt amperes).
$F^{wt}_{i,y}/F^{pv}_{i,y}$	Probabilistic distribution of $\omega^{wt}_{i,y,n}/\omega^{pv}_{i,y,n}$.
F^{α}_i/F^{β}_i	Probabilistic distribution of α_n/β_n.
$F^T_{i,y}$	Probabilistic distribution of $T_{i,y,n}$.
$b^{wt}_{i,j}/b^{pv}_{i,j}$	0 if the jth increment in size is not necessary to compose the WT/PV at node i 1 if the jth increment in size is necessary to compose the WT/PV at node i.
$c_{i,j}$	Binary indicator $c_{i,j} = a_i b_{i,j}$.
N_a/N_b	Maximum number of DGs/size increments in the feeder/at a node.
ς	Maximum-allowed voltage deviation.
$V^{in}_{i,y,n}/V^{\text{out}}_{i,y,n}$	Input/output voltage of the voltage regulator at node i in scenario n in year y.
V^{tap}	Voltage adjustment corresponding to one tap step.
$T^{\text{tap}}_{i,y,n}$	Tap position of the regulator at node i in scenario n in year y.
$T^{\max}_i/T^{\min}_i$	Maximum/minimum tap position of the regulator at node i.

Manuscript received July 03, 2013; revised December 18, 2013 and March 13, 2014; accepted May 15, 2014. Date of publication March 30, 2015; date of current version May 20, 2015. This work was supported by the U.S. Department of Energy Office of Electricity Delivery and Energy Reliability. Paper no. TPWRD-00760-2013.

Z. Wang and M. M. Begovic are with the School of Electrical and Computer Engineering, Georgia Institute of Technology, Atlanta, GA 30332 USA (e-mail: zhaoyuwang@gatech.edu; miroslav@ece.gatech.edu).

B. Chen is with the School of Industrial and Manufacturing Systems Engineering, Iowa State University, Ames, IA 50014 USA (e-mail: bokanc@iastate.edu).

J. Wang is with Argonne National Laboratory, Lemont, IL 60439 USA (e-mail: jianhui.wang@anl.gov).

Color versions of one or more of the figures in this paper are available online at http://ieeexplore.ieee.org.

Digital Object Identifier 10.1109/TPWRD.2014.2331275

f_{obj}	Value of the objective function.
ϕ/φ	Parameters of a beta distribution.
$z^*/\hat{z}$	True/approximate objective value of the original $\mathrm{SP}/\mathrm{SP}_{\mathrm{N}}$.
z_M^{*k}	Objective value approximated by SP_{Mk} in the kth MRP.
$\hat{z}_M^{*k}$	Objective value calculated by using $(\hat{a}, \hat{b}, \hat{c})$ and newly generated M scenarios in the kth MRP.
G_k	Optimality gap in the kth MRP.

I. Introduction

ENERGY DEFICIT, load growth, environmental consciousness, and constraints on building new transmission and distribution lines have created increasing interest in conservation voltage reduction (CVR) and distributed generation (DG). Both techniques can be used to save energy and reduce peak load demand.

CVR is typically utilized at substations to regulate voltage and operate feeders at the lowest acceptable voltage levels [1], [2] as shown in Fig. 1. It is known that many loads are voltage dependent and consume less power when the supplied voltage is reduced [2], [3]. CVR has been successfully implemented to reduce peak demand/energy consumption and increase the system stability margin at a number of utilities, such as NEEA and BC Hydro [4], [5]. Previous tests indicate that significant energy savings can be achieved through voltage reduction. The energy-saving effects usually range from 0.3% to 1% load reduction per 1% voltage reduction. Recent studies show that deployment of CVR on all distribution feeders in the U.S. could result in a 3.04% reduction in the annual national energy consumption [6].

The depth of voltage reduction is an important impact factor on the effectiveness of CVR. It can be seen from Fig. 1 that the level of voltage reduction is closely related to the voltage profile along the feeder. The American National Standards Institute (ANSI) standard [7] requires that the lowest voltage level remain within 5% of the nominal value. If the end-of-line (EOL) voltage is much lower than the substation voltage, then the substation voltage cannot be reduced too much, in order to maintain the EOL voltage above 114 V on a 120 V scale. Deeper voltage reduction can be achieved if the EOL voltage is maintained near the same level as the voltage at the beginning of the feeder. The most popular way to flatten the voltage profile is to place capacitor banks to provide reactive power compensation along the feeder [8], [9]. For example, [8] formulated the capacitor allocation problem as a multiobjective optimization problem to minimize voltage deviation, active power loss, as well as load and capital investment. A genetic algorithm (GA) is applied to solve that problem.

Recently, the integration of DG in distribution feeders has increased rapidly. DG has impacts on voltage profile, power quality (PQ), energy efficiency, and reliability of distribution systems. The location and size of DG units should be carefully

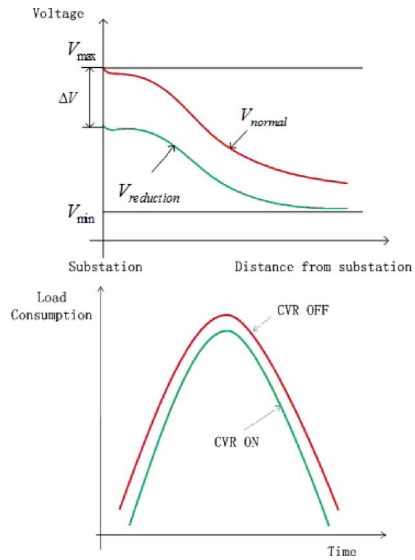

Fig. 1. Demonstration of CVR.

selected in order to take advantage of DG and limit its negative impacts on system operations. Placement of DG is typically a mixed-integer multiobjective optimization problem. A variety of objectives has been investigated in the literature, such as loss reduction [10], voltage improvement [11], reliability improvement [12], stability enhancement [13], and economic considerations [14]. However, none of these objectives optimizes the placement of DG for the purpose of voltage reduction. The integration of DG increases energy efficiency on the generation side while CVR saves energy on the demand side.

A wide range of methods has been proposed for DG placement, which can be divided into three categories: 1) sensitivity analysis [13], [15]; 2) analytical approaches [16], [17]; and intelligence algorithms (IAs) [18]–[20]. The authors of [13] used continuous power flow to identify the voltage sensitivity of each bus and then allocate DG at the most sensitive bus to improve the voltage security margin and reduce power losses. The study in [16] presented an analytical approach to identify the optimal location to place a DG to minimize power losses. IA is one of the most popular methods to determine the size and location of DG. Several works [18], [19] claimed that IAs were suitable for multiobjective problems and could achieve a near-optimal solution. However, many IAs are sensitive to algorithm settings and initial conditions. IAs converge slowly and are easy to converge to a suboptimal solution. It can be seen that all of the aforementioned existing work assumes that DG is dispatchable and controllable, which is clearly not accurate since renewable energy source (RES)-based DGs are mostly nondispatchable power sources with intermittent output. Only a few papers have considered the uncertain nature of DG outputs and load consumptions in system planning. The authors of [21] presented a probabilistic planning method to determine the optimal mix of wind, solar, and biomass units to minimize annual energy losses, but the placement of DG units is not considered. The authors of [22] allocated DGs to improve voltage stability. The probabilistic nature of the DG output was mentioned but not taken into account in the solution algorithm.

This paper presents a new method to simultaneously consider CVR and DG placement for energy saving and peak demand reduction. A novel DG placement model is proposed to minimize load consumptions of the system and maintain the voltage deviations along the feeder within a predefined range. The proposed method assumes a centralized decision maker, such as the distribution system operator, can make the DG placement plan for the CVR implementation since CVR is a measure initiated by the utilities. In order to effectively deal with the probabilistic nature of DG outputs and load consumption, the DG placement is formulated as a two-stage stochastic programming problem. The first stage includes deterministic variables. The second stage includes variables adjusted according to the uncertainties. Sample average approximation (SAA) is used to solve the two-stage stochastic formulation. SAA is a well-established method [23] and has been applied to solve power system problems effectively. Reference [24] implemented SAA to solve a generation and transmission-line expansion planning problem. The study in [25] used SAA to ensure the utilization of wind power at a certain level with high probability. It is proved that SAA converges to an optimal solution if the number of samples is large enough [26]. Since the sample size cannot be infinite in practice, we use a new method by combining the multiple replications procedure (MRP) [27] with SAA in this paper to measure the quality of the solution and find the confidence interval (CI) of the gap between the SAA solution and the optimal solution.

The major contributions of this paper are summarized as follows:

- DG placement considering that CVR is a new concept with little existing reported work;
- uncertainty and variability of DG outputs are fully considered;
- combined MRP-SAA-based solution and validation methodology.

The remainder of this paper is organized as follows: Section II discusses the relationship between CVR and DG placement, and provides the problem formulation. Section III introduces the SAA and MRP algorithms. The combined SAA and MRP techniques are developed to solve the stochastic programming problem. In Section IV, the numerical illustrative studies are presented. Section V concludes this paper with the discussion of the major findings.

II. Problem Formulation

This section introduces a widely used distribution system model and then provides the two-stage stochastic formulation of DG placement for CVR.

A. Distribution System Model

Consider a distribution system as shown in Fig. 2. There are n buses indexed by $i = 0, 1, \ldots, n$. DistFlow equations can be used to describe the complex power flows at each node i [28]

$$P_{i+1} = P_i - r_i \frac{P_i^2 + Q_i^2}{V_i^2} - p_{i+1} \tag{1}$$

$$Q_{i+1} = Q_i - x_i \frac{P_i^2 + Q_i^2}{V_i^2} - q_{i+1} \tag{2}$$

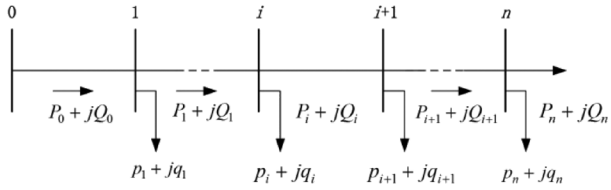

Fig. 2. Diagram of a radial distribution network.

$$V_{i+1}^2 = V_i^2 - 2(r_i P_i + x_i Q_i) + \left(r_i^2 + x_i^2\right) \frac{P_i^2 + Q_i^2}{V_i^2} \tag{3}$$

$$p_{i+1} = p_{i+1}^l - p_{i+1}^g,\ q_{i+1} = q_{i+1}^l - q_{i+1}^g. \tag{4}$$

p_i^g is generated by DG units which are subject to uncertainties. q_i^g is generated by var compensation devices, such as capacitors. The DistFlow equations are effective for radial networks. For a meshed network, it can be converted to a radial network by breaking the loops through adding dummy buses [29]. The DistFlow equations can be simplified using linearization. The linearized power-flow equations have been extensively used and justified in the literature [28]

$$P_{i+1} = P_i - p_{i+1} \tag{5}$$

$$Q_{i+1} = Q_i - q_{i+1} \tag{6}$$

$$V_{i+1} = V_i - \frac{r_i P_i + x_i Q_i}{V_0^2} \tag{7}$$

$$p_{i+1} = p_{i+1}^l - p_{i+1}^g,\ q_{i+1} = q_{i+1}^l - q_{i+1}^g. \tag{8}$$

B. Problem Formulation

The objective of CVR is to minimize total load consumption through voltage reduction. The CVR effect is closely related to load-to-voltage (LTV) sensitivity. In this study, an exponential load model is used to represent load consumption as a function of voltage. In order to effectively deal with the uncertain nature of DG outputs and load consumptions, it is necessary to formulate the problem into a stochastic optimization program. The detailed formulation is described as follows:

$$\min \sum_y \sum_n P_{y,n}^{\text{load}} \tag{9}$$

subject to

$$P_{y,n}^{\text{load}} = \sum_i p_{i,y,n}^l \tag{10}$$

$$p_{i,y,n}^l = \left(\mu_0 + \mu_1(T_{fh} - T_{i,y,n}) + \mu_2(T_{fc} - T_{i,y,n})\right) P_{i,y}^b V_{i,y,n}^{\alpha_n} \tag{11}$$

$$q_{i,y,n}^l = \left(\gamma_0 + \gamma_1(T_{fh} - T_{i,y,n}) + \gamma_2(T_{fc} - T_{i,y,n})\right) Q_{i,y}^b V_{i,y,n}^{\beta_n} \tag{12}$$

$$P_{i+1,y,n} = P_{i,y,n} - p_{i+1,y,n}^l + p_{i+1,y,n}^{g,wt} + p_{i+1,y,n}^{g,pv} \tag{13}$$

$$Q_{i+1,y,n} = Q_{i,y,n} - q_{i+1,y,n}^l + q_{i+1,y,n}^g \tag{14}$$

$$V_{i+1,y,n} = V_{i,y,n} - \frac{r_i P_{i,y,n} + x_i Q_{i,y,n}}{V_1} \tag{15}$$

$$\delta V_{i,y,n} = |V_{i,y,n} - V_1| \le \varsigma \tag{16}$$

$$p_{i,y,n}^{g,wt} = \sum_j a_i^{wt} b_{i,j}^{wt} \omega_{i,y,n}^{wt} \tag{17}$$

$$p_{i,y,n}^{g,pv} = \sum_j a_i^{pv} b_{i,j}^{pv} \omega_{i,y,n}^{pv} \tag{18}$$

$$\omega_{i,y,n}^{wt} \in F_{i,y}^{wt},\ \omega_{i,y,n}^{pv} \in F_{i,y}^{pv} \tag{19}$$

$$\alpha_n \in F_i^{\alpha},\ \beta_n \in F_i^{\beta} \tag{20}$$

$$T_{i,y,n} \in F_{i,y}^{T} \tag{21}$$

$$\sum_i a_i^{wt} + \sum_i a_i^{pv} \le N_a \tag{22}$$

$$\sum_j b_{i,j}^{wt} + \sum_j b_{i,j}^{pv} \le N_b. \tag{23}$$

In (9)–(23), the objective function (9) minimizes the total load consumptions of the system during the planning horizon. The horizon is modeled in discrete time with a 1-year time step. Constraints (10)–(12) use the combined exponential and regression models to represent the load-to-voltage and load-to-temperature relationships. The exponential and regression models have been used in the literature to represent load behaviors [30]. In this paper, we set $\mu_0 = \gamma_0 = 0.1$, $\mu_1 = \gamma_1 = 0.01$, $\mu_2 = \gamma_2 = 0.02$, and $T_{fh} = 60$ F and $T_{fc} = 70$ F [2], [31]. The parameters can be obtained using the minimum covariance determinant procedure as introduced in [31]. The values of $P_{i,1}^b$ and $Q_{i,1}^b$ used in this paper can be found in [11]. It is also assumed that the annual increasing rate of load is 1% during the planning horizon. These values can be changed according to the characteristics of a particular system and climate. Constraints (13)–(15) are linearized DistFlow equations as discussed in the previous section. Constraint (16) guarantees that the voltage deviation along the feeder is within a predefined range in order to achieve deeper voltage reduction. In this paper, it is assumed that the DGs to be connected with the system are wind turbines (WTs) and photovoltaic generators (PVs). Constraint (17) decides whether there is a WT connected with the node, while constraint (18) decides whether there is a PV connected with the node. To make the formulation more practical, it is assumed that a DG is made up by several DG units, which means the size of a DG is discrete as described by constraints (17) and (18) [21]. The sizes of a WT and PV can be represented as $\sum_j b_{i,j}^{wt} s^{wt}$ and $\sum_j b_{i,j}^{pv} s^{pv}$, respectively. Constraint (19) represents the output of one discrete increment of a WT/PV at node i, which will be discussed in the next subsection. Constraint (20) assumes that the LTV sensitivities of each node are random variables that can be represented using normal distributions [32]. In this paper, the mean and variance of F_i^{α} are set to be 1.0 and 0.08, respectively; and the mean and variance of F_i^{β} are set to be 3.6 and 0.1, respectively. All input parameters can be changed according to the available system information. Constraint (21) assumes the stochasticity of the temperature at node i can be represented by a normal distribution $F_{i,y}^T$. We assume the mean and standard deviation of $F_{i,y}^T$ are 55 F and 25 F, respectively, and the temperature distribution during the planning horizon remains the same. Constraint (22) indicates that the total number of DGs that can be connected to the system are less than or equal to N_a. Constraint (23) indicates that the total number of DG units that can be connected to a node is less than or equal to N_b. In this paper, it is assumed that $N_a = 3$ and $N_b = 6$. The purpose of DG placement is to decide the values of a_i and $b_{i,j}$. The system reconfiguration is not considered in (9)–(23) due to the low frequency of reconfigurations in current distribution systems.

Some of the above constraints can be reformulated to further reduce the nonlinearity of the problem. Equation (16) can be linearized as

$$\lambda_{i,y,n} \ge V_{i,y,n} - V_0,\ \forall i,y,n$$
$$\lambda_{i,y,n} \ge V_0 - V_{i,y,n},\ \forall i,y,n \tag{24}$$
$$\lambda_{i,y,n} \le \varsigma,\ \forall i,y,n. \tag{25}$$

Equations (17) and (18) include multiplications of two binary variables a_i and $b_{i,j}$. The bi-linear term $a_i b_{i,j}$ can be replaced by

$$c_{i,j} = a_i b_{i,j},\ c_{i,j} \le a_i,\ c_{i,j} \le b_{i,j},\ c_{i,j} \ge a_i + b_{i,j} - 1. \tag{26}$$

For a feeder with voltage regulators and capacitors, it is necessary to model these volt/var control devices as follows [33]:

$$q_{i,y,n}^{g} = X_{i,y,n}^{C} Q_i^{C} \tag{27}$$

$$V_{i,y,n}^{\text{out}} = V_{i,y,n}^{\text{in}} + \text{Tap}_{i,y,n} V^{\text{tap}} \tag{28}$$

$$\text{Tap}^{\min} \le \text{Tap}_{i,y,n} \le \text{Tap}^{\max}. \tag{29}$$

Constraint (27) represents the ON/OFF status of the capacitor at node i. Constraints (28) and (29) model the input–output voltage relationship of the voltage regulator at node i.

C. Uncertainties of DG Outputs

In this paper, two kinds of RES-based DGs are considered: WTs and PVs. The predicted wind and solar power will be used. It is known that errors always exist in prediction models. The beta function is shown to be an appropriate distribution to represent prediction errors of wind and solar power [34]. For a predicted DG output P_i^{pred} of one discrete increment of the DG at node i, the beta function can be defined by two corresponding parameters ϕ and φ

$$f_{p_i^{\text{pred}}}(x) = x^{\phi-1}(1-x)^{\varphi-1}. \tag{30}$$

The above beta function models the occurrence of real power values x when a certain prediction value P_i^{pred} has been forecasted. The shape parameters of the corresponding beta function ϕ and φ can be calculated as [34]

$$\frac{P_i^{\text{pred}}}{S_{\text{base}}} = \frac{\phi_i}{(\phi_i + \varphi_i)} \tag{31}$$

$$\sigma_i^2 = \frac{\phi_i \varphi_i}{(\phi_i + \varphi_i)^2 (\phi_i + \varphi_i + 1)}. \tag{32}$$

The relationship between the predicted power and its error variance can be represented as [34]

$$\sigma_i = 0.2 \times \frac{P_i^{\text{pred}}}{s^{wt,pv}} + 0.21. \tag{33}$$

Using the predicted DG outputs and (31)–(33), the parameters of beta functions for the current prediction data can be calculated.

The distribution and parameter settings shown before can be changed according to the available information of a system.

III. Multiple Replication Procedure

There are many methodologies to solve a stochastic optimization problem, among which, SAA is shown to be an easy and effective method [25]. The intuitive idea of SAA is to approximate the expectation term in the objective function by sampling. Based on the law of large numbers, when the size of samples is large enough, the value of the reformulated objective function converges to the value of the original objective function. At the same time, the feasible region of the reformulated problem would be equivalent to the feasible region of the original problem. However, since the sample size is finite in reality, it is important to test the quality of the solution, which is performed by the MRP in this paper. In this section, the stochastic problem will be reformulated using generated scenarios and then the combined MRP-SAA algorithm is proposed to solve the problem.

A. Scenario Generation

The first step of SAA is to generate scenarios using Monte-Carlo simulations to replace the true distributions of uncertain variables by an empirical distribution which can be obtained using the Kolmogorov-Smirnov (K-S) test with historical data. The K-S test is a nonparametric test to compare a sample with a reference probability distribution. K-S statistics quantify a distance between the empirical distribution function (EDF) of the sample and the cumulative distribution function (CDF) of the reference distribution to find the best CDF to represent the EDF. The Monte-Carlo simulation generates S scenarios for year y, each with the same probability $1/S$. Thus, there are a total of $N(S*y)$ scenarios. The objective is to obtain the minimum expected load. The general form of the problem can be written as

$$z^* = \min f(a, b, c, W) \tag{34}$$

where $f(a, b, c, W) = \sum_y \sum_n P_{y,n}^{\text{load}}|$ (11)–(29) and W represents random variables, such as WT/PV outputs, load model exponents, and temperature.

Equation (30) can be denoted as a stochastic program (SP) which depends on prior knowledge of the probability distributions of the uncertain variables. SAA is to sample N independent and identically distributed (i.i.d.) observations from the distribution of W and then solve the approximating problem (denoted as SP_N)

$$\hat{z} = \min \frac{1}{N} \sum_y \sum_{n=1}^{S} f(a, b, c, W_{y,n}). \tag{35}$$

Thus, the original problem in (9)–(23) can be reformulated to be a mixed-integer nonlinear program (MINLP) as

$$\min \frac{1}{N} \sum_y \sum_{n=1}^{S} P_{y,n}^{\text{load}} \tag{36}$$

subject to (10)–(23) and (27)–(29).

In the above MINLP formulation, variables a_i, $b_{i,j}$, and $c_{i,j}$ are first-stage variables; variables P, Q, V, p^g, and q^g are selected to be second-stage ones which change according to the uncertainty realizations. For a specific set of first-stage decisions, different costs can be associated with various scenarios. This MINLP problem can be solved by commercial solvers, such as DICOPT [35].

B. Combined MRP-SAA Algorithm

It is known from SAA that the solutions$(\hat{a}, \hat{b}, \hat{c})$ of SP_N are optimal to SP as the sample size grows into infinity. However, since $(\hat{a}, \hat{b}, \hat{c})$ is obtained by solving SP_N with a finite sample size in practice, it is necessary to test the quality of the solution, which is performed by the MRP in this paper.

The true optimal solution of SP is (a^*, b^*, c^*) with the optimal value z^* $(z^* = \min f(a, b, c, W))$. While $(\hat{a}, \hat{b}, \hat{c})$ is obtained from N scenarios in solving SP_N, we generate new samples with M new scenarios (M is usually larger than or equal to N) by K times in MRP. Here, we define the individual problem in the $K*M$ samples as $SP_{Mk}, k = 1, \ldots, K$. We can then obtain a new objective value z_M^{*k} by using the same SAA procedure for each SP_{Mk}. Since an upper bound on the optimality gap of $(\hat{a}, \hat{b}, \hat{c})$ in the kth MRP (denoted as G_k) can be estimated by

$$\frac{1}{M} \sum_{m=1}^{M} f\left(\hat{a}, \hat{b}, \hat{c}, W_m^k\right) - \min \frac{1}{M} \sum_{m=1}^{M} f\left(a, b, c, W_m^k\right) \tag{37}$$

where the M scenarios are i.i.d. from the distribution of W, $(1/M)\sum_{m=1}^{M} f(\hat{a}, \hat{b}, \hat{c}, W_m^k)$ is calculated by using $(\hat{a}, \hat{b}, \hat{c})$ in the newly generated M scenarios. MRP is to repeat this procedure for multiple times (K times in this paper) and construct the confidence interval (CI) for the optimality gap. The form of the CI can be describes as

$$P\left(f(\hat{a}, \hat{b}, \hat{c}, W) - z^* \le \varepsilon\right) \approx 1 - \alpha \tag{38}$$

where ε is the CI width, and $1 - \alpha$ is the confidence (e.g., 0.95).

Fig. 3 shows the flowchart of the combined SAA and MRP algorithm. The complete MRP-SAA steps can be described as follows.

- Step 1) Generate N scenarios and use SAA to solve the SP_N problem as defined in (31) and obtain the candidate solution $(\hat{a}, \hat{b}, \hat{c})$.
- Step 2) Generate M scenarios and use SAA to solve the SP_M problem and obtain the solution (a^{*k}, b^{*k}, c^{*k}) and the objective value z_M^{*k}.
- Step 3) Use the solution of the SP_N problem $(\hat{a}, \hat{b}, \hat{c})$ and the M scenarios to calculate $\hat{z}_M^{*k} = (1/M)\sum_{m=1}^{M} f(\hat{a}, \hat{b}, \hat{c}, W_m^k)$.
- Step 4) Calculate the optimality gap $G_k(\hat{a}, \hat{b}, \hat{c}) = \hat{z}_M^{*k} - z_M^{*k}$.
- Step 5) Repeat Steps 2)–4) for $k = 1, 2, \ldots, K$.
- Step 6) Calculate the mean and variance of the optimality gap by $\overline{G} = (1/K)\sum_{k=1}^{K} G_k(\hat{a}, \hat{b}, \hat{c})$ and $s^2 = (1/K-1)\sum_{k=1}^{K}(G_k(\hat{a}, \hat{b}, \hat{c}) - \overline{G})^2$, then the one-sided CI of the optimality gap is $[0, \overline{G} + t_{K-1,\alpha^s}/\sqrt{K}]$, where $t_{K-1,\alpha}$ is the α-quantile of the t-distribution with $K-1$ degrees of freedom, and we denote the CI as $[0, \theta]$, where $\theta = \overline{G} + t_{K-1,\alpha^s}/\sqrt{K}$.

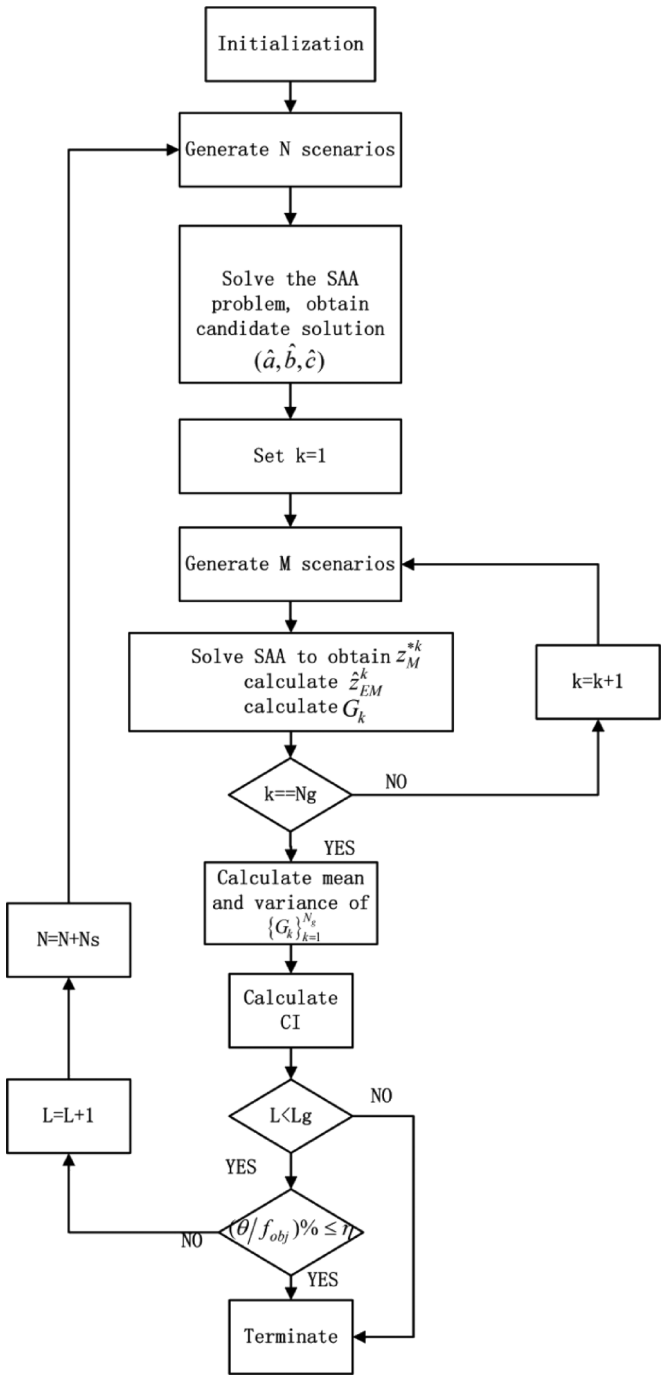

Fig. 3. Flowchart of the combined MRP and SAA algorithm.

Step 7) If the number of iterations exceeds the maximum value Lg, terminate the process; otherwise, go to Step 8).

Step 8) If $(\theta/f_{\rm obj}) \times 100\%$ is less than a predefined value η, terminate the process; otherwise, increase the number of scenarios by N_s and go to Step 1); η is defined to be 5% in this paper.

Since most of the previous work in DG placement uses deterministic optimization, it is necessary to show how much improvement can be achieved if the stochastic nature of DG is taken into account. For the problem defined in (28), we replace the random variable ω by its expected value, and then the expected value problem (EV), which is a deterministic optimization problem, can be defined as

$$\mathrm{EV} = \min f(a, b, c, \bar{W}) \tag{39}$$

where $\bar{W} = E(\bar{W})$ denotes the expectation of $\bar{W}$. The expected value solution can be defined as $(\bar{a}, \bar{b}, \bar{c})$. The expected results of using the EV solution can be represented as

$$\mathrm{EEV} = \frac{1}{N'} \sum_{h=1}^{N'} f(\bar{a}, \bar{b}, \bar{c}, W_h). \tag{40}$$

EEV measures the performance of $(\bar{a}, \bar{b}, \bar{c})$, allowing second-stage decision variables to be chosen optimally as functions of $(\bar{a}, \bar{b}, \bar{c})$ and W. In order to measure how good or, more frequently, how bad the decision $(\bar{a}, \bar{b}, \bar{c})$ is, when compared with $(\hat{a}, \hat{b}, \hat{c})$, Monte Carlo simulation is used. We generate N' scenarios (N' is usually larger than N). The solution of the SP_N problem $(\hat{a}, \hat{b}, \hat{c})$ is used in each of the N' scenarios to calculate $f(\hat{a}, \hat{b}, \hat{c}, \omega_h)$, $h = 1, \ldots, N'$. The difference between EEV and the MC result can be defined as

$$D = \mathrm{EEV} - \frac{1}{N'} \sum_{h=1}^{N'} f(\hat{a}, \hat{b}, \hat{c}, W_h). \tag{41}$$

Since the formulation is a minimization problem, the larger the D, the more the stochastic programming outperforms deterministic programming.

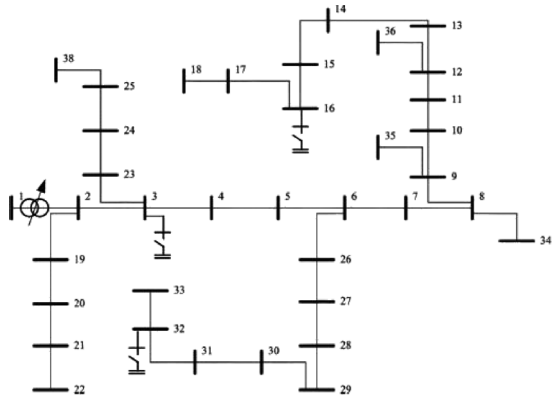

Fig. 4. The 37-bus distribution system.

IV. Case Study

A. DG Placement Results

The proposed methodology has been examined on the 37-bus radial distribution network as shown in Fig. 4. Assume the substation transformer is with ±5% tap range and 10 tap positions. Switched capacitors are installed at nodes 3, 16 and 32, each is 30 kVar. Details about the test system can be found in [11]. The power base is 10 MVA, the voltage base is 12.66 kV. Table I shows the base case (without DG and CVR) of the test system.

It is assumed that one size increment of a WT and a PV is 0.01 p.u. MATLAB is used to generate scenarios of WT/PV output

TABLE I
BASE CASE OF THE TEST SYSTEM

Max. Voltage Deviation (p.u.)	Active Loss (p.u.)	Total Active Load (p.u.)	Substation Voltage (p.u.)
0.09	0.028	0.3715	1.05

TABLE II
DG PLACEMENT RESULTS

Node No.	Type	Size (p.u.)
8	WT	0.01
	PV	0.01
13	WT	0.03
	PV	0.01
31	WT	0.03
	PV	0.02

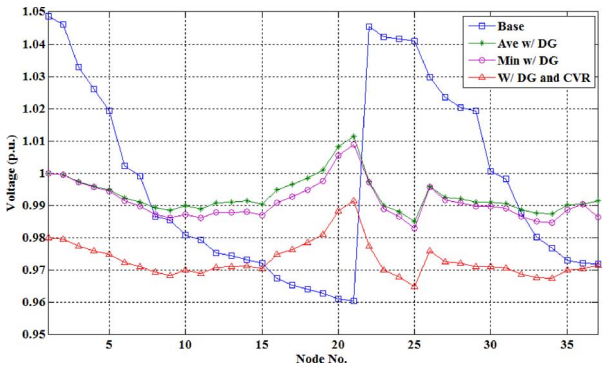

Fig. 5. Voltage profiles.

to calculate the candidate solution for the 37-node network. The planning horizon is assumed to be 10 years and 200 scenarios are generated for each year ($S = 200$), thus there are totally 2000 scenarios ($N = 2000$). The two stage stochastic program defined in (36) is solved using GAMS.

Table II shows the placement results. The DG penetration level can be defined as the total DG generation divided by the system peak load. For the planning results, the DG penetration level is 30%. Fig. 5 shows the voltage profiles of the test system. There are four profiles in the figure: 1) base case without DG or CVR; 2) average voltages of all N scenarios without voltage reduction; 3) minimum voltages of all N scenarios without voltage reduction; and 4) average voltages of all N scenarios with CVR. In the base case, there is almost no potential for voltage reduction since the largest voltage deviation is 0.09 p.u., and the substation voltage is set to be 1.05 p.u. in order to make sure the EOL voltage is within the standard. After DG integration, the voltage profiles are improved largely. The voltage deviations are within 0.03 p.u. even for the worst case, which provides enough space for implementing voltage reduction. The substation voltage can be reduced from 1.05 to 0.98 p.u. with optimal placement of wind turbines.

Fig. 6 shows the active total load consumptions of three cases during the planning horizon (one year consists of 8760 h): 1) the base case without DG or CVR; 2) the case with stochastic optimal DG placement but without voltage reduction; 3) the case with stochastic optimal DG placement and with CVR. It can be seen that the load consumptions of the base case are much higher than the other two cases. This shows the effectiveness of

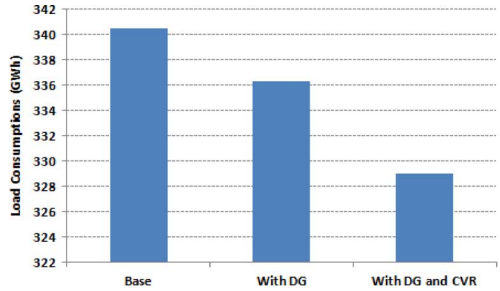

Fig. 6. Active load consumption.

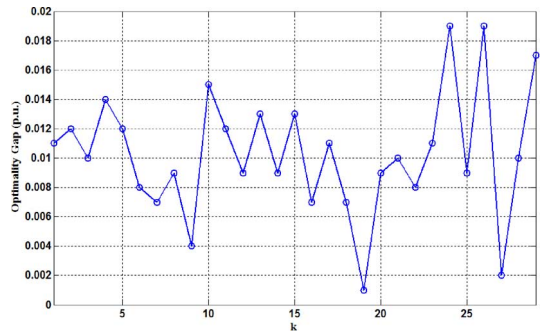

Fig. 7. Optimality gap in MRP.

the stochastic optimal DG placement in improving the system operation. Moreover, significant load consumptions can be reduced by CVR, which shows that more energy savings can be achieved if the implementation of CVR and the placement of DG are considered simultaneously.

B. MRP Results

As discussed in section IV, MRP can be used to test the stability and quality of the candidate solutions. The candidate solution is tested against 29 samples ($K = 29$), each with a sample size of 2500 ($M = 2500$). The optimality gaps are shown in Fig. 7, the mean value of gaps is $\overline{G} = 0.007586$, the standard deviation is $s = 0.008231$. The CI for the optimality gap is [0, 0.0102] with $\alpha = 0.05$, which means that there is a chance of 95% that the optimality gap is within the CI. Thus, the candidate solution of the stochastic programming is very stable and of high quality.

C. Compared With Deterministic Results

As discussed in Section III, we generate $N' = 3000$ scenarios, and use $\bar{W}$ in solving the deterministic optimal DG placement. The formulation of the deterministic optimal problem is similar to (9)–(29). The only difference is that all random variables are substituted by their mean values. The problem is solved by GAMS. Recall we denote the solution of this deterministic problem as EV.

The DG placement results are: WTs should be placed at nodes 6, 8, and 30, with the sizes of 0.01, 0.02, and 0.03 p.u., respectively, and PVs should be placed at nodes 6, 8, and 30, with the sizes of 0.01, 0.02, and 0.01 p.u. As shown in (41), Monte Carlo simulation is run to compare the performances of the deterministic placement and the stochastic placement. Fig. 8 shows the comparison results. The deterministic solution is worse when

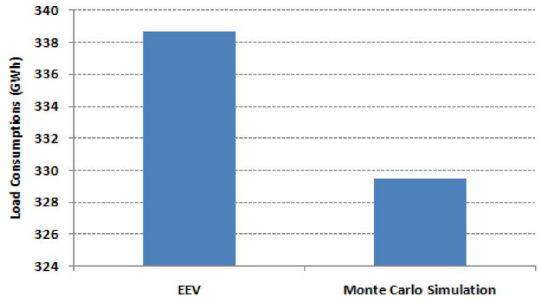

Fig. 8. Comparison of EEV and Monte Carlo simulation.

wind turbine output is stochastic. Considering the probabilistic nature of DG output in practice, the proposed stochastic programming is more suitable and realistic.

V. Conclusion

This paper presents a new DG placement strategy for implementing CVR. The DG placement is defined as a stochastic optimization problem to enable the distribution system to realize deeper voltage reduction to decrease load consumptions. In order to deal with the uncertain nature of DG outputs and load consumptions, a combined SAA-MRP-based algorithm is developed to obtain the optimal solution. The quality of the optimal solution is validated by calculating its confidence interval using MRP. The case studies show the effectiveness of the proposed formulation and prove that significant power reduction can be achieved, if the integration of DG and implementation of CVR is considered simultaneously.

Acknowledgment

The submitted manuscript has been created by UChicago Argonne, LLC, Operator of Argonne National Laboratory ("Argonne"). Argonne, a U.S. Department of Energy Office of Science laboratory, is operated under Contract No. DE AC02-06CH11357. The U.S. Government retains for itself, and others acting on its behalf, a paid-up nonexclusive, irrevocable worldwide license in said article to reproduce, prepare derivative works, distribute copies to the public, and perform publicly and display publicly, by or on behalf of the Government.

References

[1] D. Lauria, "Conservation voltage reduction (CVR) at Northeast Utilities," *IEEE Trans. Power Del.*, vol. 2, no. 4, pp. 1186–1191, Oct. 1987.
[2] Z. Wang and J. Wang, "Review on implementation and assessment of conservation voltage reduction," *IEEE Trans. Power Syst.*, vol. 29, no. 3, pp. 1306–1315, May 2014.
[3] Z. Wang, M. Begovic, and J. Wang, "Analysis of conservation voltage reduction effects based on multistage SVR and stochastic process," *IEEE Trans. Smart Grid*, vol. 5, no. 1, pp. 431–439, Jan. 2014.
[4] T. L. Wilson, "Measurement and verification of distribution voltage optimization results," in *Proc. IEEE Power Energy Soc. Gen. Meeting*, 2010, pp. 1–9.
[5] D. Kirshner, "Implementation of conservation voltage reduction at Commonwealth Edison," *IEEE Trans. Power Syst.*, vol. 5, no. 4, pp. 1178–1182, Nov. 1990.
[6] J. F. K. Schneider, F. Tuffner, and R. Singh, Evaluation of conservation voltage reduction (CVR) on a national level, 2010. [Online]. Available: http://www.pnl.gov/main/publications/external/technical_reports/PNNL-19596.pdf
[7] *Electric Power Systems and Equipment Voltage Ratings (60 Hz)*, ANSI Standard C84.1-1995, ANSI, 1995.
[8] B. Milosevic and M. Begovic, "Capacitor placement for conservative voltage reduction on distribution feeders," *IEEE Trans. Power Del.*, vol. 19, no. 3, pp. 1360–1367, Jul. 2004.
[9] C. McCarthy and J. Josken, "Applying capacitors to maximize benefits of conservation voltage reduction," in *Proc. Rural Elect. Power Conf.*, 2003, pp. C4-1–C4-5.
[10] N. Acharya, P. Mahat, and N. Mithulananthan, "An analytical approach for DG allocation in primary distribution network," *Int. J. Elect. Power Energy Syst.*, vol. 28, pp. 669–678, 2006.
[11] D. Singh and K. Verma, "Multiobjective optimization for DG planning with load models," *IEEE Trans. Power Syst.*, vol. 24, no. 1, pp. 427–436, Feb. 2009.
[12] D. Zhu, R. P. Broadwater, K. S. Tam, R. Seguin, and H. Asgeirsson, "Impact of DG placement on reliability and efficiency with time-varying loads," *IEEE Trans. Power Syst.*, vol. 21, no. 1, pp. 419–427, Feb. 2006.
[13] H. Hedayati, S. Nabaviniaki, and A. Akbarimajd, "A method for placement of DG units in distribution networks," *IEEE Trans. Power Del.*, vol. 23, no. 3, pp. 1620–1628, Jul. 2008.
[14] Z. Wang, B. Chen, J. Wang, J. Kim, and M. Begovic, "Robust optimization based optimal DG placement in microgrids," *IEEE Trans. Smart Grid*, to be published.
[15] M. Ettehadi, H. Ghasemi, and S. Vaez-Zadeh, "Voltage stability-based DG placement in distribution networks," *IEEE Trans. Power Del.*, vol. 28, no. 1, pp. 171–178, Jan. 2013.
[16] C. Wang and M. H. Nehrir, "Analytical approaches for optimal placement of distributed generation sources in power systems," *IEEE Trans. Power Syst.*, vol. 19, no. 4, pp. 2068–2076, Nov. 2004.
[17] H. D. Quoc and N. Mithulananthan, "Multiple distributed generator placement in primary distribution networks for loss reduction," *IEEE Trans. Ind. Electron.*, vol. 60, no. 4, pp. 1700–1708, Apr. 2013.
[18] K.-H. Kim, Y.-J. Lee, S.-B. Rhee, S.-K. Lee, and S.-K. You, "Dispersed generator placement using fuzzy-GA in distribution systems," in *Proc. IEEE Power Eng. Soc. Summer Meeting*, 2002, pp. 1148–1153.
[19] N. S. Rau and Y.-H. Wan, "Optimum location of resources in distributed planning," *IEEE Trans. Power Syst.*, vol. 9, no. 4, pp. 2014–2020, Nov. 1994.
[20] R. S. Rao, S. V. L. Narasimham, M. R. Raju, and A. S. Rao, "Optimal network reconfiguration of large-scale distribution system using harmony search algorithm," *IEEE Trans. Power Syst.*, vol. 26, no. 3, pp. 1080–1088, Aug. 2011.
[21] Y. Atwa, E. El-Saadany, M. Salama, and R. Seethapathy, "Optimal renewable resources mix for distribution system energy loss minimization," *IEEE Trans. Power Syst.*, vol. 25, no. 1, pp. 360–370, Feb. 2010.
[22] R. S. Al Abri, E. F. El-Saadany, and Y. M. Atwa, "Optimal placement and sizing method to improve the voltage stability margin in a distribution system using distributed generation," *IEEE Trans. Power Syst.*, vol. 28, no. 1, pp. 326–334, Feb. 2013.
[23] J. R. Birge and F. Louveaux, *Introduction to Stochastic Programming*. Berlin, Germany: Springer-Verlag, 1997.
[24] P. Jirutitijaroen and C. Singh, "Reliability constrained multi-area adequacy planning using stochastic programming with sample-average approximations," *IEEE Trans. Power Syst.*, vol. 23, no. 2, pp. 504–513, May 2008.
[25] Q. Wang, Y. Guan, and J. Wang, "A chance-constrained two-stage stochastic program for unit commitment with uncertain wind power output," *IEEE Trans. Power Syst.*, vol. 27, no. 1, pp. 206–215, Feb. 2012.
[26] Q. Wang, J. Wang, and Y. Guan, "Stochastic unit commitment with uncertain demand response," *IEEE Trans. Power Syst.*, vol. 28, no. 1, pp. 562–563, Feb. 2013.
[27] G. Bayraksan and D. P. Morton, "Assessing solution quality in stochastic programs," *Math. Program.*, vol. 108, no. 2–3, pp. 495–514, Sep. 2006.
[28] M. E. Baran and F. F. Wu, "Network reconfiguration in distribution systems for loss reduction and load balancing," *IEEE Trans. Power Del.*, vol. 4, no. 2, pp. 1401–1407, Apr. 1989.
[29] M. Haque, "Efficient load flow method for distribution systems with radial or mesh configuration," *Proc. Inst. Elec t. Eng., Gen., Transm. Distrib.*, vol. 143, no. 1, pp. 33–38, Jan. 1996.
[30] W. Price, S. Casper, C. Nwankpa, R. Bradish, H. Chiang, and C. Concordia *et al.*, "Bibliography on load models for power flow and dynamic performance simulation," *IEEE Power Eng. Rev.*, vol. 15, no. 2, pp. 523–538, Feb. 1995.

[31] Global Energy Partners, Walnut Creek, CA, USA, Distribution efficiency initiative, Tech. rep. 08-192, Jun. 2008. [Online]. Available: http://www.smartgridnews.com/artman/uploads/1/sgnr_2007_08011.pdf
[32] K. Srinivasan and C. Lafond, "Statistical analysis of load behavior parameters at four major loads," *IEEE Trans. Power Syst.*, vol. 10, no. 1, pp. 387–392, Feb. 1995.
[33] H. A. Mostafa, R. El-Shatshat, and M. M. A. Salama, "Multi-objective optimization for the operation of an electric distribution system with a large number of single phase solar generators," *IEEE Trans. Smart Grid*, vol. 4, no. 2, pp. 1038–1047, Jun. 2013.
[34] T. Niknam, M. Zare, and J. Aghaei, "Scenario-based multiobjective volt/var control in distribution networks including renewable energy sources," *IEEE Trans. Power Del.*, vol. 27, no. 4, pp. 2004–2019, Oct. 2012.
[35] I. E. Grossmann, J. Viswanathan, A. Vecchietti, R. Raman, and E. Kalvelagen, "GAMS/DICOPT: A discrete continuous optimization package," *Math. Meth. Appl. Sci.*, vol. 24, no. 11, pp. 649–664, Jul. 2001.

Zhaoyu Wang (S'13) received the B.E. and M.S. degrees in electrical engineering from Shanghai Jiaotong University, Shanghai, China, in 2009 and 2012, respectively, and the M.S. degree in electrical and computer engineering from the Georgia Institute of Technology, Atlanta, GA, USA, in 2012, where he is currently pursuing the Ph.D. degree in electrical and computer engineering.

In 2013, he was a Research Aide Intern at Decision and Information Sciences Division, Argonne National Laboratory, Argonne, IL, USA. His current research interests include microgrids, volt/var control, demand response and energy conservation, system modeling and identification, as well as stochastic optimization in power systems.

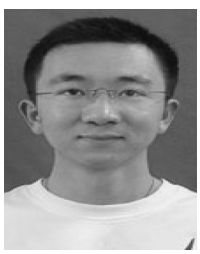

Bokan Chen received the B.S. degree in electronics and information engineering from Huazhong University of Science and Technology, Wuhan, China, in 2011 and the M.S. degree in industrial and manufacturing systems engineering at Iowa State University, Ames, IA, USA, where he is currently pursuing the Ph.D. degree in industrial engineering.

His research interests include optimization theories and their applications.

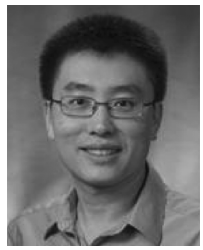

Jianhui Wang (M'07–SM'12) received the Ph.D. degree in electrical engineering from Illinois Institute of Technology, Chicago, IL, USA, in 2007.

Presently, he is a Computational Engineer with the Decision and Information Sciences Division at Argonne National Laboratory, Argonne, IL, USA. He is an Affiliate Professor at Auburn University, Auburn,. AL, and an Adjunct Professor at University of Notre Dame, Notre Dame, IN. He is an editor of the IEEE TRANSACTIONS ON POWER SYSTEMS, the IEEE TRANSACTIONS ON SMART GRID, an Associate Editor of the *Journal of Energy Engineering*, an Editor of the IEEE Power and Energy Society Letters, and an Associate Editor of *Applied Energy*. He is also the editor of Artech House Publishers Power Engineering Book Series

Dr. Wang is the chair of the IEEE Power & Energy Society (PES) Power System Operation Methods Subcommittee. He is the recipient of the IEEE Chicago Section 2012 Outstanding Young Engineer Award.

Miroslav M. Begovic (S'87–M'89–SM'92–F'04) is Professor and Chair of the Electric Energy Technical Interest Group in the School of Electrical Engineering, Georgia Institute of Technology, Atlanta, GA, USA. His studies focus on analysis, monitoring, and control of voltage stability and applications of phasor measurements in electrical power systems. His research concentrates on real-time monitoring systems for control of power system dynamics, protective relaying, distribution network operation, and distributed resources in energy systems.

Prof. Begovic is a former Chair of the IEEE PES Emerging Technologies Coordinating Committee and has contributed to technical activities within IEEE and CIGRE. He is a member of Sigma Xi, Tau Beta Pi, Phi Kappa Phi, and Eta Kappa Nu, and currently serves as President of IEEE Power and Energy Society. He is a member of the IEEE Power and Energy Society Power System Relaying Committee.